Determination of the Rate Constant for Chain Insertion into Poly(methyl methacrylate)-*block*-poly(methacrylic acid) Micelles by a Fluorescence Method

Carl K. Smith† and Guojun Liu*

Department of Chemistry, University of Calgary, 2500 University Drive, NW, Calgary, Alberta, Canada T2N 1N4

Received September 7, 1995; Revised Manuscript Received December 11, 1995⊗

ABSTRACT: Poly(methyl methacrylate)-*block*-poly(methacrylic acid) (PMMA-*b*-PMAA) with and without pyrene labels attached to the end of the PMAA block have been synthesized and characterized. These polymers formed micelles with PMAA as the core in ethyl acetate/methanol mixtures when the ethyl acetate volume fraction was higher than 80%. After mixing a micelle solution of PMMA-*b*-PMAA without pyrene labels, i.e., polymer I, with a unimer solution of the sample with pyrene, i.e., polymer II, the fluorescence intensity $I_{Py}(t)$ of pyrene increased with time. This was caused by the insertion of the pyrene group of polymer II chains into the rigid core of polymer I micelles. The pyrene fluorescence quantum yield is higher in a more rigid environment due to the reduced quenching of pyrene fluorescence by oxygen and the possible suppression of certain nonradiative deactivation pathways. A kinetic model has been proposed for describing the chain insertion process. Fitting the experimental fluorescence intensity data using the derived expression for $I_{Py}(t)$ allowed the first determination of the rate constant k_n for diblock copolymer chain insertion into micelles.

I. Introduction

In a micellar system, single chain exchange between the unimer pool and micelles, the breakdown of large micelles into small ones (fission), and the formation of large micelles from small ones (fusion) may all occur simultaneously.[1,2] Of all the processes, the single chain exchange process as denoted by the following equation:

$$M_n \underset{k_n}{\overset{k_{-n}}{\rightleftharpoons}} M_{n-1} + U \qquad (1)$$

is the fastest, as recently argued by Halperin and Alexander.[3] In eq 1, M_n and M_{n-1} are micelles with n and $n - 1$ unimer chains, respectively; U denotes a unimer chain; and k_n and k_{-n} are unimer insertion and expulsion rate constants. At equilibrium, k_n and k_{-n} are related by

$$k_n[M_{n-1}][U] = k_{-n}[M_n] \qquad (2)$$

The rate constant for chain expulsion from micelles, i.e., k_{-n}, is a key parameter sought by scientists using diblock copolymer micelles as drug carriers for controlled drug delivery.[4] In cases when the drugs are chemically attached to the core block, k_{-n} is important as the rate of chain expulsion determines the rate of drug release. Rate constants k_n and k_{-n} also shed light on the rate of diblock copolymer brush buildup, as polymer brushes,[5−8] self-assembled structures of diblock copolymers at a solid substrate and a solution interface, bear close resemblance to the structure of diblock micelles.

Despite the fundamental importance of k_n or k_{-n}, the study of micelle chain exchange kinetics has been rare in the past. Halperin and Alexander[3] have recently derived scaling relations between k_{-n} and the lengths of two blocks of a diblock copolymer. Some experimental studies have been carried out, and the results have been analyzed in the spirit of the Aniansson and Wall (A−W) theory,[9] originally developed for small-molecule surfactant micelles. According to the A−W theory, the concentration of unimers or micelles or their equivalence should relax after a "perturbation" to their new equilibrium values with two relaxation times T_1 and T_2, where $T_1 < T_2$. Assuming that the chain exchange process is much faster than the micelle fusion and fission processes, Aniansson and Wall related T_1 and T_2 to k_{-n} and micelle characteristic parameters such as the average aggregation number $\bar{n}_a$ and the variance σ in $\bar{n}_a$.

Although the relaxation kinetics of diblock micelles has been found to follow a two-stage mechanism in agreement with the A−W theory, rate constants such as k_{-n} have so far not been determined. The difficulty has been in establishing the equivalence between the experimentally determined T_1 and T_2 and those discussed by A−W.

Wang et al.[10] and Procházka et al.[11] labeled diblock copolymers with fluorescence donors and acceptors and prepared micelles from the samples. Micelles containing chains otherwise identical except with different labels were then mixed. Due to chain exchange after micelle mixing, donors residing in the same micelles as acceptors may transfer electronic excitation energy to acceptors via the dipole−dipole energy transfer mechanism.[12] Energy transfer decreases the fluorescence intensity of the donor but increases that of the acceptor, although the donor is selectively excited in the process. The experimental data of Wang et al. and Procházka et al., i.e., the variation in the fluorescence intensity $I(t)$ of the donor as a function of time, could be fitted with a sum of two exponential terms to obtain T_1 and T_2. T_1 and T_2 were not used to calculate k_{-n} as $I(t)$ was, by no means, a linear function of parameters such as the number of acceptor-labeled chains entering a micelle consisting primarily of donor-labeled chains. Instead, $I(t)$ was a complex function of the efficiency of energy migration among donor groups, the number and locations of donors and acceptors in a micelle, and the rate constant for energy transfer etc.

† Now at Schlumberger Cambridge, High Cross, Madingley Road, Cambridge, U.K. CB3 0EL.

⊗ Abstract published in *Advance ACS Abstracts,* February 1, 1996.

0024-9297/96/2229-2060$12.00/0

In addition to the aforementioned complication, most of the previous studies were plagued by the use of large perturbations. The use of large perturbations, such as the sudden change in solvent composition[13] or temperature[14] to cause micelle formation from a solution without micelles or vice versa, makes the experimental detection of the relaxation process easier but the A−W theory inapplicable.

In this paper, we report the first experimental determination of k_n. For this, we have used poly(methyl methacrylate)-*block*-poly(methacrylic acid) (PMMA−*b*-PMAA) and fluorene- and pyrene-labeled PMMA-*b*-PMAA or Fl-PMMA-*b*-PMAA-Py:

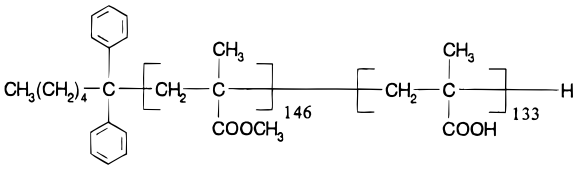

PMMA-*b*-PMAA or Polymer I

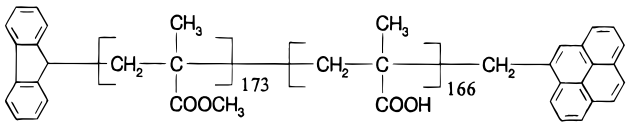

Fl-PMMA-*b*-PMAA-Py or Polymer II

The experiment involved mixing a micelle solution of polymer I with a unimer solution of polymer II in a solvent selectively poor for the PMAA block. After mixing, unimers of polymer II incorporated into micelles of polymer I. This was accompanied by a gradual increase in the fluorescence intensity of pyrene. Pyrene fluorescence increased due to the reduced efficiency of pyrene fluorescence quenching by oxygen and the possible suppression of some nonradiative decaying processes of excited pyrene inside the PMAA core. From analyzing the pyrene fluorescence intensity variation data, we obtained k_n.

In the next section, the detailed experimental design will be discussed and an analytical expression for the increase in pyrene fluorescence intensity $I_{Py}(t)$ as a function of time will be given. Experimental procedures will be presented in section III. Treatment of experimental results using theoretical equations is shown in section IV, and some conclusions are drawn in section V.

II. Discussion of the Experiment and Theory

More Detailed Features of the Experiment. As mentioned in the Introduction, our experiment involved mixing a micellar solution of polymer I with a unimer solution of polymer II. The use of a unimer solution of polymer II is important as it is the change in the environment of pyrene, i.e., from the unimer surroundings to the PMAA core of a micelle, which leads to the increase in the fluorescence intensity.

We then assume, as was done in a previous paper by one of us on the design of experiments for micelle chain exchange kinetic studies,[15] that the experiment is performed using a higher molar micelle concentration c_M^0 of polymer I than the molar polymer concentration c_y^0 of polymer II. This makes the probability for finding micelles, at the end of the experiment, containing more than one polymer II chain negligible and leads to a great simplification of our later mathematical derivation for an expression for $I_{Py}(t)$. The molar micelle concentration c_M^0 can be tuned using

$$c_M^0 = \frac{c - c^*}{\bar{n}_a} \tag{3}$$

where $\bar{n}_a$ denotes the average micelle aggregation number, c the molar polymer I concentration, and c^* the critical micelle concentration. For the convenience of later discussion, we assume that $c_y^0 = ac^*$, where a is less than 1.

Lastly, we assume that the structural difference between polymers I and II is so small that the two types of chains distribute randomly in a micellar system at long times after the mixing.

Qualitative Analysis of the Experiment in Terms of the Aniansson−Wall Model. Immediately after mixing, unimer concentration [U] is $(1 + a)c^*/2$, as [U] $= ac^*$ for the polymer II solution and [U] $= c^*$ for the polymer I micelle solution and the volume increases by a factor of 2 due to the mixing of two solutions of equal volume. The negative deviation of [U] from c^* leads to the rapid dissociation of unimers from the existing micelles until the total unimer concentration is c^* again. In terms of the Aniansson−Wall description,[9] the new supply of unimers is provided by the stepwise dissociation, i.e., one chain at a time, of chains from micelles. This initial adjusting period, characterized by T_1, is short and the total number of micelles remains approximately constant during this time domain.

At time $t \approx T_1$, the average size of the micelles in the system is smaller than their equilibrium size due to the dissociation of some unimer chains in the initial stage. In the next phase, a small number of micelles will thus undergo stepwise disintegration and the majority will undergo stepwise uptaking of unimers to regain their equilibrium size. It is mainly in this stage that polymer II chains, existing initially almost exclusively as unimers, are inserted into polymer I micelles. Since chain insertion mainly occurs on the time scale characterized by T_2, we expect, in terms of the aniansson−Wall model, that analysis of our experimental results should lead to a single relaxation time, i.e., T_2. The exact relation describing the relaxation in $I_{Py}(t)$ will be derived in the next subsections.

Kinetic Model. In a micelle system, micelle fusion, fission, and single chain insertion into and expulsion from micelles, as described in the Introduction, all occur simultaneously. Although Halperin and Alexander[3] argued for the dominance of the process of single chain insertion or expulsion, this conviction has recently been challenged by Mattice and co-workers as their Monte Carlo simulations demonstrated that micelle fusion and fission played a dominant role at high micellar concentrations, e.g., >5% in volume.[16] In addition to chain exchange involving polymer II chains, chain exchange involving polymer I also occurs. A micellar system is thus very complex.

Fortunately, most of the processes described above can be ignored since they do not contribute to any variation in $I_{Py}(t)$. Processes which do not involve polymer II chains can be ignored. Chain exchange involving polymer II due to micelle fusion and fission can be ignored as the transferring of a polymer II chain from one micelle to another does not change $I_{Py}(t)$ either.

The only processes which change $I_{Py}(t)$ are

$$M_n + \text{〰}Py \underset{1/(n+1)k_{-n}}{\overset{k_n}{\rightleftharpoons}} M_nPy \quad (4)$$

In assuming the validity of eq 4, we have neglected the probability for the incorporation of two or more polymer II chains into the same micelle. This assumption can be satisfied by making c_y^0 much smaller than c_M^0. In eq 4, 〰Py represents a unimer of polymer II; M_n denotes a micelle with n polymer I chains. The factor $1/(n+1)$ before k_{-n} in eq 4 accounts for the fact that every unimer chain, either polymer I or II, has an equal chance to exit a micelle and that there is only one polymer II chain out of a total of $(n+1)$ chains in a micelle M_nPy. Equation 4 applies to micelles of all sizes.

In the extreme of a sharp distribution of micelle aggregation numbers, we can assume that all micelles have the same aggregation number $\bar{n}_a$. Since the concentration of micelles is relatively high, e.g., $c_M^0 \geq c^*$, the average aggregation number of micelles, even immediately after solution mixing, is close to $\bar{n}_a$. In terms of the close-association model, eq 4 is now rewritten as

$$M + \text{〰}Py \underset{1/(\bar{n}_a+1)k_{-n}}{\overset{k_n}{\rightleftharpoons}} MPy \quad (5)$$

where M stands for a micelle.

Kinetic Equations. The rate of *MPy* formation from eq 5 is

$$\frac{d[MPy]}{dt} = k_n[M][\text{〰}Py] - \frac{1}{\bar{n}_a+1}k_{-n}[MPy] \quad (6)$$

where [M] stands for the molar micelle concentration at time t, [MPy] the concentration of micelles containing polymer II chains, and [〰Py] the concentration of polymer II unimers at time t.

To simplify notation, we let

$$x = [MPy] \quad (7)$$

Due to the no more than one polymer II chain per micelle assumption

$$[M] = c_M^0 - x \quad (8)$$

and

$$[\text{〰}Py] = c_y^0 - x \quad (9)$$

Inserting eqs 7, 8, and 9 into eq 6 and simplifying yields

$$\frac{dx}{dt} = k_n x^2 - b_1 x + b_2 \quad (10)$$

where

$$b_1 = k_n(c_M^0 + c_y^0) + k_{-n}/(\bar{n}_a + 1) \quad (11)$$

and

$$b_2 = k_n c_M^0 c_y^0 \quad (12)$$

The solution for eq 10 is

$$x = \frac{2k_n c_M^0 c_y^0(1 - e^{-kt})}{b_1 + k - (b_1 - k)e^{-kt}} \quad (13)$$

where

$$k = (b_1^2 - 4k_n b_2)^{1/2} \quad (14)$$

Pyrene Fluorescence Intensity as a Function of Time. We assume that the fluorescence quantum yields of pyrene groups associated with unimers and micelles be ϕ_u and ϕ_m, respectively. The fluorescence intensity of pyrene at t after mixing is then

$$I_{Py}(t) = \kappa[\phi_m x + \phi_u(c_y^0 - x)] \quad (15)$$

where κ is a parameter dependent on the instrument settings and the initial concentration of polymer II but is constant throughout a mixing experiment. Equation 15 reduces to

$$I_{Py}(0) = \kappa\phi_u c_y^0 \quad (16)$$

at $t = 0$. Inserting eqs 16 and 13 into eq 15 and rearranging yields

$$I_{Py}(t) - I_{Py}(0) = \frac{\kappa'(1 - e^{-kt})}{b_1 + k - (b_1 - k)e^{-kt}} \quad (17)$$

where $\kappa' = 2\kappa(\phi_m - \phi_u)k_n c_M^0 c_y^0$. Thus, pyrene fluorescence intensity increases with time if $\phi_m > \phi_u$.

Equation 17 clearly suggests that the relaxation in $I_{Py}(t)$ can be described by a single rate constant k but k is a complex function of k_n, k_{-n}, c_M^0, c_y^0, and $\bar{n}_a$. $I_{Py}(t)$ data can be fitted with eq 17 to determine b_1 and k. These values can then be used to calculate k_n and k_{-n} from

$$k_n = \left(\frac{b_1^2 - k^2}{4c_M^0 c_y^0}\right)^{1/2} \quad (18)$$

and

$$k_{-n} = (\bar{n}_a + 1)[b_1 - k_n(c_M^0 + c_y^0)] \quad (19)$$

For k_n and k_{-n} calculation, we need experimental values of c_y^0, c_M^0, and $\bar{n}_a$.

III. Experimental Section

Materials. Fluorene was recrystallized three times from methanol and three times from hexane. Lithium chloride was dried under vacuum prior to use. Methyl methacrylate (MMA) was washed with 10% sodium hydroxide solution to remove the stabilizer, then washed with water, and dried over $MgSO_4$. Just before the polymerization, MMA was distilled over CaH_2 and then triethylaluminum. *tert*-Butyl methacrylate (Polymer Laboratories) was passed through activated aluminum oxide (acidic, Brockmann I) and distilled over CaH_2 twice under reduced pressure prior to use in polymerization.

1-Pyrenemethanol. The compound was synthesized by sodium borohydride reduction of 1-pyrenecarboxaldehyde (Aldrich, 99%) following a literature method.[17] The pure product was obtained after recrystallization from cyclohexane three times.

1-(Bromomethyl)pyrene. This compound was synthesized from 1-pyrenemethanol also following a literature method.[18] The methanol product (1.9 g) was dissolved in CCl_4 (125 mL), and PBr_3 (0.4 mL) was then added. The reaction was allowed to proceed for 2 h at 55−60 °C before being terminated with the addition of 1 mL of methanol. The CCl_4 solution was subsequently washed three times with a 10% $NaHCO_3$ aqueous solution, three times with distilled water, and once with a saturated NaCl solution. The organic layer

was dried over Na_2CO_3. After filtration, the solvent was removed. The product was recrystallized from a mixture of CCl_4 and hexane.

Polymerization. Polymer II was synthesized according to the following scheme. The PMAA block was derived from the hydrolysis of poly(*tert*-butyl methacrylate) (PTBMA).

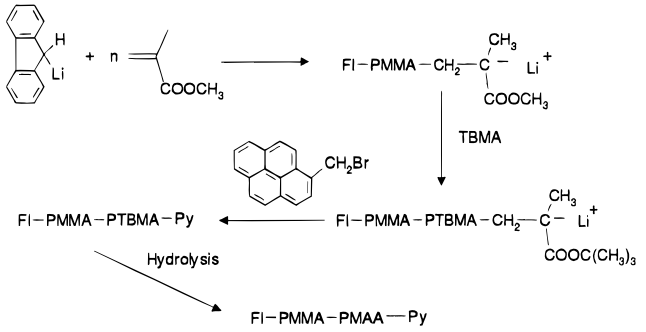

Fluorenyllithium was prepared by reacting equal molar amounts of fluorene and *n*-butyllithium (1.6 M, 0.1 mL) at 0 °C in THF for 5 min. Lithium chloride was then added to improve the polydispersity of the polymer to be prepared, and the reaction mixture was cooled to −78 °C. Methyl methacrylate was polymerized at this temperature for 0.5 h before *tert*-butyl methacrylate (TBMA) was added. The polymerization of TBMA proceeded for 6 h and was terminated with 1-(bromomethyl)pyrene (1.5 equiv). The excess terminator was removed by precipitating Fl-PMMA-*b*-PTBA from THF by adding pentane slowly.

To hydrolyze the *tert*-butyl groups, Fl-PMMA-*b*-PTBMA-Py was dissolved in dry dichloromethane. Excess trimethylsilyl iodide (Aldrich, 97%) was then added to this solution under argon at room temperature, and the mixture was stirred for 45 min before the solvent and excess trimethylsilyl iodide were removed under reduced pressure.[19] After dissolving in THF, the polymer solution was poured into methanol containing a catalytic amount of 10% HCl aqueous solution.[20] The mixture was stirred for 10 min and the polymer was precipitated out by pouring in a NaS_2O_5 aqueous solution. The dried, hydrolyzed diblock was purified further by dissolving in 1:1 methanol/ethyl acetate and precipitation from the solution phase by the gradual addition of freshly distilled diethyl ether.

Polymer I was prepared by following similar procedures except that MMA polymerization was initiated by (1,1-diphenylhexyl)lithium obtained from reacting equal molar amounts of *n*-butyllithium and freshly distilled 1,1-diphenylethylene (Aldrich, 97%). The polymerization of TBMA was terminated by the addition of methanol.

Steady-State Fluorescence. Steady-state fluorescence measurements were made on a Photon Technologies Alphascan instrument with a 75 W lamp. The steady-state spectra were not corrected. For the kinetic experiments, vigorous stirring was maintained throughout an experiment. Pyrene was excited at 326 nm and the pyrene emission was measured at 387 nm. To minimize instrument drift, the pyrene fluorescence intensity of a standard sample, consisting of a copolymer micelle solution of the same composition but with polymers I and II thoroughly mixed, was always measured immediately after each sample measurement. $I_{Py}(t)$ used were actually the intensity ratios between a sample and a standard at time t.

Time-Resolved Fluorescence. Fluorescence lifetimes measurements were taken on a Photon Technologies LS1 time-correlated single photon counting spectrometer. Pyrene was excited at 326 or 343 nm and the fluorescence emission was monitored at 387 nm. The fluorescence experiments were done under ambient atmospheric conditions.

UV−Visible Spectroscopy. UV measurements were carried out on a Hewlett-Packard 8450A diode array single-beam spectrometer. The labeling efficiency of 1-(bromomethyl)-pyrene was determined by using 1-pyrenemethanol as the standard [$\epsilon(342\ \text{nm}) = 4.34 \times 10^4\ \text{cm}^{-1}\cdot\text{M}^{-1}$].

Gel Permeation Chromatography. The PMAA blocks of polymers I and II were methylated with 3-methyl-1-*p*-tolyltriazene to convert them to PMMA before GPC analysis.[21,22] Analysis of the methylated polymers I and II, i.e., PMMA and Fl-PMMA-Py, was done with a Varian 5000 liquid chromatograph instrument equipped with Zorbax 60S, 300S, and 1000s columns using THF as the eluent and monitored by a refractive index detector. Monodisperse PMMA standards (Polysciences, Inc.) were used to calibrate this instrument.

Proton NMR. A delay time of 20 *s* between pulses was employed for running all samples. Precursors polymers PMMA-*b*-PTBA were solubilized and analyzed in CD_2Cl_2, and polymers I and II were analyzed in CD_3OD. The relative amounts of the PMMA and PTBA blocks were established by ratioing the peak intensity of the methyl group bonded to the carboxyl group of MMA (3.70−3.53 ppm) to that of the *tert*-butyl group of PTBMA (1.50−1.41 ppm). The degree of hydrolysis was determined from the ratios of the integrated areas of the methyl ester protons (3.70−3.53 ppm) to that of the remaining *tert*-butyl groups (1.50−1.41 ppm).

Dynamic Light Scattering. The hydrodynamic radii R_h of micelles were determined, at 21 ± 0.5 °C, by photon correlation spectroscopy using an ALV spectrometer equipped with an ALV-5000 full digital correlator (280 channels) over the time range from 10^{-7} to 10^3 s. Both the incident beam, from an Addas Nd-YAG laser with emission at 532 nm, and the scattered beam were polarized vertical to the scattering plane. The typical micelle concentration used was between 0.3 and 1 mg/mL, and the scattering angle, θ, was between 15 and 45°.

The intensity autocorrelation function was analyzed by an inverse Laplace transformation using a program called Contin to obtain the distribution $P(\omega)$ in and the average $\langle\omega\rangle$ of relaxation times ω. ω is related to the relaxation rate Dq^2 by

$$\omega = 1/(Dq^2) \tag{20}$$

where D is the diffusion coefficient of micelles, and q, the magnitude of the scattering vector, is related to the wavelength of the laser beam λ and the refractive index n_r of the solvent by

$$q = \frac{4\pi n_r}{\lambda}\sin(\theta/2) \tag{21}$$

At a given D, the hydrodynamic radius R_h has calculated using

$$R_h = \frac{kT}{6\pi\eta D} \tag{22}$$

or

$$R_h = \frac{kTq^2\omega}{6\pi\eta} \tag{23}$$

where kT refers to the thermal energy at temperature T and η the zero-shear-rate viscosity of the solvent used, which we determined experimentally. The distribution in R_h, $P(R_h)$, was obtained using $P(R_h) \propto P(\omega)$.

In cases of a binary solvent mixture, n_r was calculated from the refractive indices n_1 and n_2 of the individual solvents using[23]

$$(1/\varrho)(n_r - 1) = (w_1/\rho_1)(n_1 - 1) + (w_2/\rho_2)(n_2 - 1) \tag{24}$$

where w_1 and w_2 are the weight fractions of components 1 and 2, respectively, and ρ_1 and ρ_2 are their densities. The refractive indices of THF, cyclohexane, and chloroform at 532 nm have been approximated by 1.4050, 1.4266, and 1.4459, their values at the sodium emission line.[24]

Viscometry Measurements. The flow times of solvents and polymer micelle solutions were measured using a Cannon-Ubbelohde type viscometer immersed in a water bath equilibrated at 21.0 °C. The viscosity of a solution or a solvent is assumed to be linearly proportional to its flow time. The reduced viscosity η_{red} of a solution is then calculated using

$$\eta_{red} = \frac{t_f - t_f^0}{t_f^0 c} \quad (25)$$

where t_f and t_f^0 are the flow times of the solution and the solvent, respectively.

Preparation of Micelle Solutions. The micelles were formed by the slow dropwise addition of ethyl acetate to a solution of either polymer I or II in a mixture of methanol and ethyl acetate (v/v = 1:1), under vigorous stirring. These micelle solutions were stirred at 40−45 °C for at least 4 h for establishing micelle size distribution equilibrium before any physical measurements.

IV. Results and Discussion

Characterization of the Polymers. Illustrated in Figure 1 is the ^{1}H NMR spectrum of PMMA-*b*-PTBMA, the precursor to polymer I. The three broad peaks between 0.9 and 1.2 ppm are due to the protons of the methyl groups next to the PMMA nad PTBMA backbones. The peak between 1.7 and 2.0 ppm is due to the backbone methylene unit in PMMA and PTBMA. From ratioing the peak intensity of the *tert*-butyl protons, at ∼1.45 ppm, of PTBMA to that of the protons, at ∼3.6 ppm, of the methyl group bonded to the carboxyl group of PMMA, we obtained a MMA to TBMA molar ratio, *n*/*m*, of 1.11. Similarly, we obtained the *n*/*m* value of 1.05 for polymer II.

After hydrolysis, we still found 5% of residual *tert*-butyl groups by ^{1}H NMR analysis of polymers I and II in CD_3OD. Due to this small amount of residual TBMA units in the final polymer, the behaviors observed from these polymers may not be typical of those of a pure PMMA-*b*-PHEMA copolymer.

GPC results of methylated polymers I and II are shown in Table 1. In both cases, sample molar mass distributions are narrow. Combining GPC and NMR results, we obtained the number of MMA and MAA units, *n* and *m*, of 146 and 133 for polymer I and 173 and 166 for polymer II.

The UV−vis absorption spectrum of a polymer II sample at the concentration of 1.53 mg/mL in THF is illustrated in Figure 2. Fluorene has strong absorption peaked at 292 and 302 nm, respectively. Above 310 nm, only pyrene absorbs with maxima at 312, 326, and 342 nm. Based on the assumption that the terminal pyrenyl group of polymer II has the same molar extinction coefficient, i.e., 4.3×10^4 $M^{-1}\cdot cm^{-1}$, at 342 nm in THF as 1-pyrenemethanol at 344 nm, we determined a pyrene termination efficiency of 51%.

Illustrated in Figure 3 are the fluorescence emission spectra of polymer II in ethyl acetate/methanol mixtures with the ethyl acetate contents of 50 and 90%, respectively, when fluorene was selectively excited at 290 nm. As is obvious from Figure 3, the fluorene emission in the 290−365 nm region is well resolved from the pyrene emission in the 370−450 nm region. No peak was observed above 450 nm, which suggests that excimer formation from pyrene was not favorable. This is quite reasonable considering that the pyrene concentration is low and that the viscosity inside a micellar core is high.

I_{Py}/I_{Fl} Upon Micellization. The emission intensity of pyrene relative to that of fluorene is considerably higher in the solvent mixture was 90% ethyl acetate than that with 50% ethyl acetate. The I_{Py}/I_{Fl} values for polymer II at the constant concentration of 0.117 mg/mL in different solvent mixtures are plotted as a function of methanol content in Figure 4. As the methanol content decreased to ∼20%, I_{Py}/I_{Fl} suddenly increased steeply. This must have been due to micelle formation, and 0.117 mg/mL represents the critical micelle concentration of polymer II at the ethyl acetate content of ∼80%.

That I_{Py}/I_{Fl} increases upon micellization can be appreciated from a few considerations. First, the efficiency of energy transfer from fluorene to pyrene may increase upon micellization. This increase may result from the

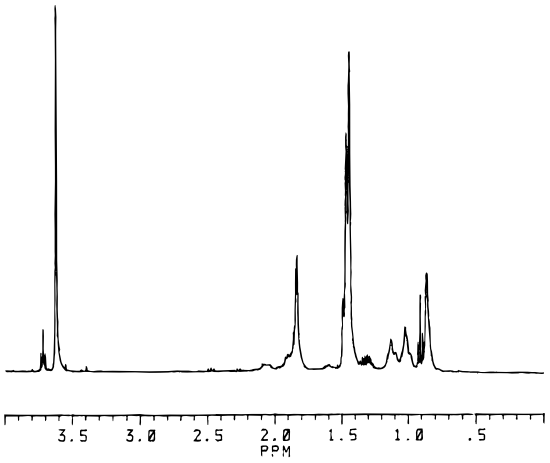

Figure 1. ^{1}H NMR spectrum of PMMA-*b*-PTBMA, the precursor for polymer I, in CD_2Cl_2.

Table 1. Characterization Results of the Diblock Copolymers

sample	*n*/*m* by NMR[a]	$\bar{M}_n$/(g/mol) by GPC[b]	$\bar{M}_w/\bar{M}_n$ by GPC[b]
polymer I	1.11	2.88×10^4	1.12
polymer II	1.05	3.48×10^4	1.09

[a] Obtained from analyzing PMMA-*b*-PTBMA. [b] Results obtained after the PMAA blocks were methylated with 3-methyl-1-*p*-tolyltriazene.

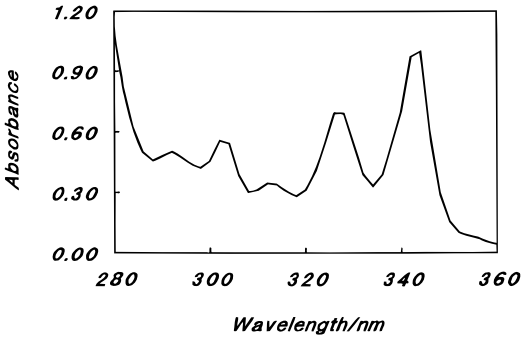

Figure 2. UV absorption spectrum of polymer II at the concentration of 1.53 mg/mL in THF.

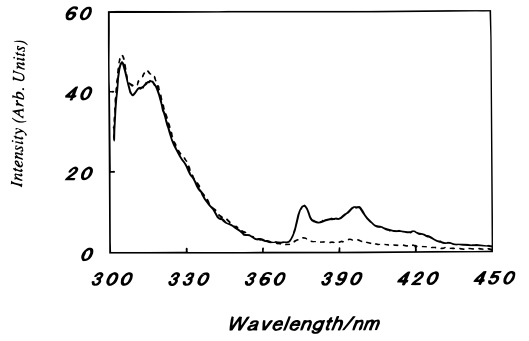

Figure 3. Fluorescence emission spectra of polymer II in ethyl acetate/methanol mixtures with 90% (—) and 50% (- - -) of ethyl acetate, respectively. In both cases, fluorene was selectively excited at 290 nm.

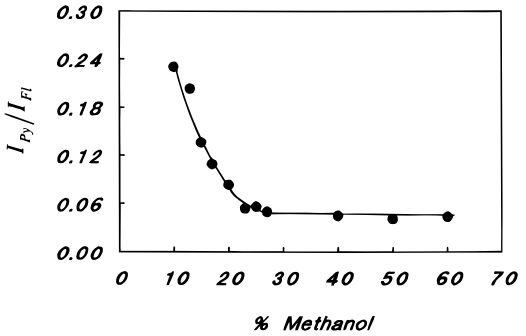

Figure 4. Increase in I_{Py}/I_{Fl} as a function of the volume fraction of methanol in methanol/ethyl acetate mixtures for polymer II at the concentration of 0.117 mg/mL.

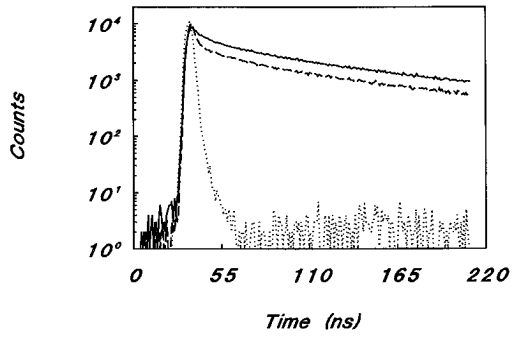

Figure 5. Pyrene fluorescence intensity decay data for polymer II at the concentrations of 0.56×10^{-2} (- - -) and 1.49×10^{-2} (—) mg/mL, respectively, in methanol/ethyl acetate mixtures with the ethyl acetate content of 85%. (···) represents the lamp profile.

possible energy transfer from a fluorene group of one chain to a pyrene group of another chain. Energy transfer efficiency is further increased due to the possible energy migration among fluorene groups of different chains. Through energy migration, an exciton can be transported to a fluorene group which is closest to a pyrene group. Then, I_{Py} increases due to the reduced quenching of pyrene fluorescence by oxygen and the possible suppression of certain nonradiative decaying channels of excited pyrene molecules.

Critical Micelle Concentration. As discussed before, our experiment required the mixing of a unimer solution of polymer II with a micelle solution of polymer I. We intended to carry out the micelle kinetic studies at the ethyl acetate contents of 85 and 90%, respectively. The critical micelle concentrations of polymer II at these solvent compositions were determined to guide the preparation of unimer solutions of polymer II.

As micelles form, we expect that the fluorescence quantum yield of pyrene or its fluorescence lifetime to increase. Illustrated in Figure 5 are the time-resolved fluorescence intensity decay data of pyrene of polymer II when pyrene was excited at 326 and its emission monitored at 387 nm. The polymer II concentrations used were 0.56×10^{-2} and 1.49×10^{-2} mg/mL, respectively, and the ethyl acetate content was 85%. As micelles form, the contribution from the short-time components diminished and thus the average fluorescence lifetime $\langle\tau\rangle$ increased.

Pyrene fluorescence decay data $F(t)$ at different concentrations were fitted by the deconvolution method[25] using a sum of three exponential terms:

$$F(t) = \sum_{i=1}^{3} a_i \exp(-t/\tau_i) \tag{26}$$

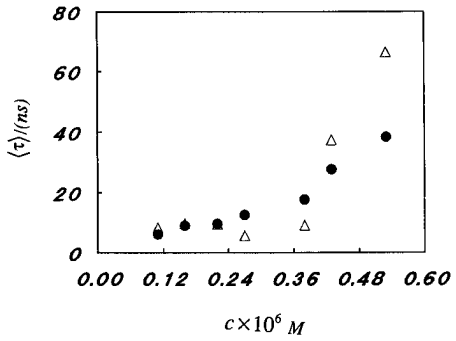

Figure 6. Increase in the average fluorescence lifetime $\langle\tau\rangle$ of pyrene as a function of polymer II concentration at the ethyl acetate contents of 85% (Δ) and 90% (●), respectively.

Table 2. Characterization Results of Polymer I and II Micelles in Different Solvent Mixtures

sample	$1/\omega$ (10^4 s^{-1})	$q \times 10^{-5}$ (cm^{-1})	η (cP) of solvent	R_h (Å)	$[\eta]$ (mL/g)	$\bar{n}_a$
Ethyl Acetate/Methanol = 90/10						
polymer I	2.58	3.121	0.436	189	9.1	171
polymer II	2.32	3.121	0.436	210		
Ethyl Acetate/Methanol = 85/15						
polymer I	2.48	3.116	0.433	198	10.4	172
polymer II	2.25	3.116	0.433	217		

where a_i and τ_i are the amplitude coefficient and the lifetime of each fitting term, respectively. The average fluorescence lifetime τ was calculated using

$$\langle\tau\rangle = \sum_{i=1}^{3} a_i\tau_i \tag{27}$$

Shown in Figure 6 is the variation of $\langle\tau\rangle$ with polymer II concentration at the ethyl acetate contents of 85 and 90%, respectively. In the solvent with 85% ethyl acetate, $\langle\tau\rangle$ starts to increase at the concentration $\sim 4 \times 10^{-7}$ M, which is the cmc. Similarly, the cmc is $\sim 2.3 \times 10^{-7}$ M in the solvent with 90% ethyl acetate. As ethyl acetate content increased, the cmc decrease was expected.

Average Molecular Mass of Polymer I Micelles M_M. The calculation of c_M^0 requires the use of the average molar mass M_M of polymer I micelles. We did not use static light scattering for this purpose. Instead, we used

$$M_M = \frac{10\pi N_{av} R_h^3}{3[\eta]} \tag{28}$$

where $[\eta]$ is the intrinsic viscosity of micelle solutions in a given solvent mixture, R_h the polymer hydrodynamic radius, and N_{av} Avogadro's constant.

As M_M is related to the molar mass M of individual polymer chains by

$$M_M = \bar{n}_a M \tag{29}$$

knowing M_M allowed the immediate calculation of the average aggregation number $\bar{n}_a$. In all our calculations, M was replaced by the weight-average molar mass $\bar{M}_w$ of each polymer.

For R_h measurement, we used dynamic light scattering, and the results are summarized in Table 2. Due to the slightly higher n and m numbers for polymer II, R_h are larger for polymer II in both solvent mixtures, in agreement with theoretical predictions.[5] Shown in Figure 7 are the R_h distributions, from treating DLS

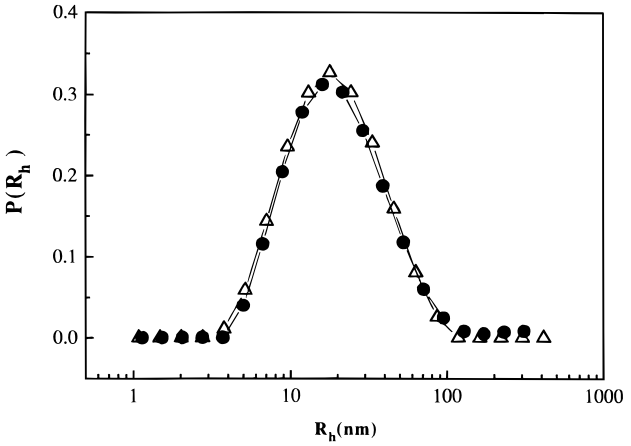

Figure 7. R_h distribution for polymer I micelles in methanol/ethyl acetate mixtures with the ethyl acetate contents of 90% (Δ) and 85% (●), respectively.

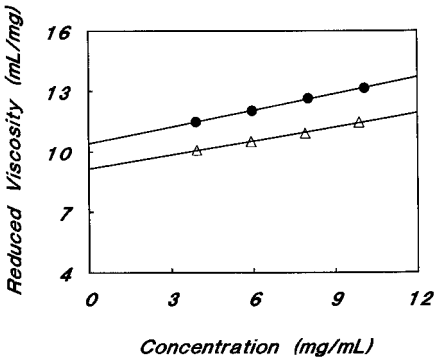

Figure 8. Variation in the reduced viscosity of polymer I in methanol/ethyl acetate mixtures with the ethyl acetate contents of 90% (Δ) and 85% (●) as a function of polymer concentration.

data with the Contin program, for polymer I in the solvents with the ethyl acetate contents of 85 and 90%, respectively.

Shown in Figure 8 is the variation in the reduced viscosity η_{red} of polymer I micelles as a function of polymer concentration c in solvents with the ethyl acetate contents of 85 and 90%, respectively. Extrapolating to zero concentration, the intrinsic viscosities of 9.1 and 10.4 mL/g were obtained for polymer I micelles in the two solvent mixtures. Using eq 24, the corresponding micelle molar masses were calculated to be 4.64×10^6 and 4.76×10^6 g/mol, respectively. The $\bar{n}_a$ values were then 171 and 172.

The aggregation numbers are the same, within experimental error, for 90 and 85% ethyl acetate solutions. That diblock copolymer micelle aggregation numbers did not vary significantly with the further addition of the poor solvent, i.e., ethyl acetate in this case, is in agreement with our observation for another system.[26]

Chain Exchange Rate Constants k_n. In the solvent with 90% ethyl acetate, three sets of kinetic experiments with different c_M^0 and c_y^0 values, shown in Table 3, were performed. To examine the effect of solvent composition, we have also carried out a kinetic run at the ethyl acetate content of 85%. In all cases, c_y^0 were lower than c^* and c_M^0.

Since only 51% polymer II chains were labeled with pyrene, c_y^0 was calculated using

$$c_y^0 = 0.51 \times c_{II}/2 \tag{30}$$

Table 3. Chain Exchange Rate Constants k_{-n} Determined under Different Experimental Conditions

run	c_M^0 (M)	c_y^0 (M)	k (s^{-1})	k_n ($s^{-1}\cdot M^{-1}$)	χ^2
		Ethyl Acetate/Methanol = 90/10			
1	2.97×10^{-7}	5.46×10^{-8}	4.90×10^{-4}	2.02×10^3	2.1×10^{-3}
2	2.97×10^{-7}	3.12×10^{-8}	5.40×10^{-4}	2.03×10^3	2.5×10^{-3}
3	1.80×10^{-7}	3.09×10^{-8}	3.99×10^{-4}	2.68×10^3	1.5×10^{-3}
		Ethyl Acetate/Methanol = 85/15			
1	3.01×10^{-7}	5.41×10^{-8}	9.13×10^{-4}	3.70×10^3	1.3×10^{-3}

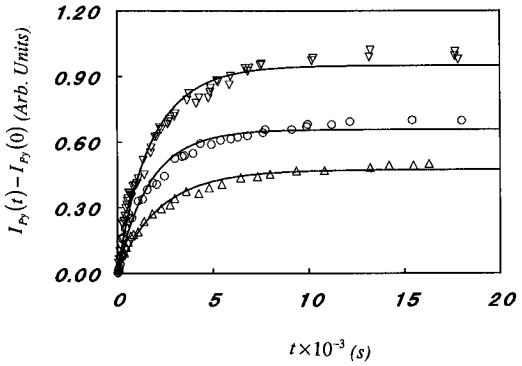

Figure 9. Pyrene fluorescence intensity increase with time after polymer I micelles were mixed with a polymer II unimer solution. The experiment was carried in an ethyl acetate/methanol mixture with 90% ethyl acetate. c_M^0 and c_y^0 are (▽) 2.97×10^{-7} and 5.46×10^{-8} M, (○) 2.97×10^{-7} and 3.12×10^{-8} M, and (Δ) 1.80×10^{-7} and 3.09×10^{-8} M, respectively. The solid curves represent the best fit to the experimental data.

where 2 accounts for the dilution factor when an equal volume of polymer I and II solutions were mixed.

The experimental steady-state fluorescence intensity data $I_{Py}(t)$ of pyrene as a function of time after sample mixing are shown in Figure 9. We attempted the treatment of the data with eq 17 using κ', b_1, and k as the fitting parameters. Unfortunately, the resulting k values were negative in some cases, which had no physical meaning. This suggested that our experimental data could not be fitted with eq 17 which contained three fitting parameters.

To reduce the number of fitting parameters in eq 17, we used

$$k_{-n} \approx k_n c^* \tag{31}$$

following from eq 2. Inserting eq 31 into eq 11 and noting that $\bar{n}_a$ is ~200, the second term on the right-hand side of eq 11 is thus negligible. Neglecting this term, eq 17 simplifies to

$$I_{Py}(t) - I_{Py}(0) = \frac{\kappa'(1 - e^{-kt})}{1 - \frac{c_y^0}{c_M^0} e^{-kt}} \tag{32}$$

where

$$k = (c_M^0 - c_y^0)k_n \tag{33}$$

and

$$\kappa' = \kappa(\phi_m - \phi_u)c_y^0 \tag{34}$$

As c_y^0/c_M^0 is accessible experimentally, the treatment of experimental $I_{Py}(t) - I_{Py}(0)$ data with eq 32 only requires two fitting parameters.

The fitting of the experimental data with eq 32 was achieved by minimizing

$$\chi^2 = (1/N) \sum_{i=1}^{N} [I_{ex}(i) - I_{th}(i)]^2 \qquad (35)$$

where N is the total number of data points in a set; $I_{ex}(i)$ and $I_{th}(i)$ stand for the experimental pyrene fluorescence intensity data and those calculated from eq 32, respectively. To enable a meaningful comparison between the resultant χ^2 from different runs, $I_{ex}(i)$ were all normalized with respect to the highest $I_{ex}(i)$ value in each data set. $I_{ex}(i)$ or $I_{Py}(t)$ are plotted in Figure 9 not to the same scale to facilitate the viewing of the experimental data.

The fits between eq 32 and experimental data were reasonable, within experimental error. The resultant k values are all shown in Table 3, and the k_n values were calculated using eq 34. In the same solvent mixture, that the resultant k_n values did not change significantly with the use of different c_M^0 and c_y^0 values suggests the validity of our model. The fact that k_n increased as the ethyl acetate content decreased is in agreement with the expectation that the PMAA core might be more swollen in the 85% ethyl acetate mixture.

V. Conclusions

PMMA-*b*-PMAA and Fl-PMMA-*b*-PMAA-Py with similar n and m numbers have been synthesized and characterized. These polymers were found to form micelles in methanol/ethyl acetate mixtures with the ethyl acetate content greater than 80%. The aggregation numbers of these micelles were determined by the combined measurement of the hydrodynamic radius and intrinsic viscosity of the micelles. Upon micelle formation from polymer II, pyrene fluorescence lifetime and I_{Py}/I_{Fl} increased. From monitoring the increase in the average fluorescence lifetime of pyrene with polymer II concentration, we determined the critical micelle concentrations of 2.3×10^{-7} and 3.8×10^{-7} M in ethyl acetate/methanol mixtures with the ethyl acetate contents of 90 and 85%, respectively.

The proposed new method only probes the single chain exchange processes. Using this method, we have, for the first time, obtained the rate constant k_n for chain insertion into micelles. In ethyl acetate/methanol mixtures with 90% ethyl acetate, k_n have been determined from three different runs. The k_n values were found to be, within experimental error, independent of the c_M^0 and c_y^0 used, as expected. k_n increased as the ethyl acetate content decreased to 85%, in agreement with the expection that the PMAA core is more swollen in this mixture. Our method will be useful for verifying scaling relations developed by Halperin and Alexander[3] for k_{-n}.

Acknowledgment. The authors wish to thank NSERC of Canada for financial support of this research. Dr. J. Tao is acknowledged for carrying out the dynamic light scattering studies. We are indebted to Dr. G. Fytas, at the Institute of Electronic Structure and Laser, Iraklion, Crete, for allowing us to use their dynamic light scattering facility.

References and Notes

(1) Hunter, R. J. *Foundations of Colloid Science*, Clarendon Press: Oxford, 1986.
(2) Tuzar, Z.; Kratochvil, P. *Surf. Colloid Sci.* **1992**, *15*, 1.
(3) Halperin, A.; Alexander, S. *Macromolecules* **1989**, *22*, 2403.
(4) Cammas, S.; Kataoka, K. Site Specific Drug Carriers: Polymeric Micelles as High Potential Vehicles for Biologically Active Molecules. Presented at NATO ASI, July 31−August 11, 1995, Turkey.
(5) Halperin, A.; Tirrell, M.; Lodge, T. P. *Adv. Polym. Sci.* **1992**, *100*, 31.
(6) Milner, S. *Science* **1991**, *251*, 905.
(7) Liu, G.; Hu, N.; Xu, X.; Yao, H. *Macromolecules* **1994**, *27*, 3892.
(8) Liu, G.; Xu, X.; Skupinska, K.; Hu, N.; Yao, H. *J. Appl. Polym. Sci.* **1994**, *53*, 1699.
(9) (a) Aniansson, E. A. G.; Wall, S. N. *J. Phys. Chem.* **1974**, *78*, 1024. (b) *Ibid.* **1975**, *79*, 986. (c) Aniansson, E. A. G.; Wall, S. N.; Almgren, M.; Hoffman, H.; Kielmann, I.; Ulbricht, W.; Zana, R.; Lang, J.; Tondre, C. *Ibid.* **1976**, *80*, 905.
(10) Wang, Y.; Kausch, C. M.; Chu, M.; Quirk, R. P.; Mattice, W. L. *Macromolecules* **1995**, *28*, 904.
(11) Procházka, K.; Bednár, B.; Mukhtar, E.; Svoboda, P.; Trnëná, J.; Almgren, M. *J. Phys. Chem.* **1991**, *95*, 4563.
(12) Förster, Th. In *Modern Quantum Chemistry*; Sinanöglu, O., Ed.; Academic Press: New York, 1965.
(13) Bednár, B.; Edwards, K.; Almgren, M.; Tormod, S.; Tuzar, Z. *Makromol. Chem., Rapid Commun.* **1988**, *9*, 785.
(14) Honda, C.; Hasegawa, Y.; Hirunuma, R.; Nose, T. *Macromolecules* **1994**, *27*, 7660.
(15) Liu, G. *Can. J. Chem.* **1995**, *73*, 1995.
(16) Mattice, W. L. Monte Carlo Simulation of Diblock Chain Exchange Kinetics. Presented at NATO ASI, July 31−August 11, 1995, Turkey.
(17) Duhamel, J.; Yekta, A.; Hu, Y. Z.; Winnik, M. A. *Macromolecules* **1992**, *25*, 7024.
(18) Al-Takrity, E. T. B. Ph.D. Thesis, University of Sussex, 1989.
(19) Jung, M. E.; Lyster, M. A. *J. Am. Chem. Soc.* **1976**, *99*, 968.
(20) Hirao, A.; Kato, H.; Yamaguchi, K.; Nakahama, S. *Macromolecules* **1992**, *25*, 7024.
(21) Blumstein, R.; Murphy, G. J.; Blumstein, A.; Watterson, A. C. *J. Polym. Sci., Polym. Lett. Ed.* **1973**, *15*, 21.
(22) Liu, G.; Guillet, J. E.; Al-Takrity, E. T. B.; Jenkins, A. D.; Walton, D. R. M. *Macromolecules* **1990**, *23*, 1393.
(23) Huglin, M. B. *Light Scattering from Polymer Solutions*; Academic Press: London, 1971.
(24) Weast, R. C. *CRC Handbook of Chemistry and Physics*, 70th ed.; CRC Press: Boca Raton, FL, 1990.
(25) O'Connor, D. V.; Phillips, D. *Time-Correlated Single Photon Counting*; Academic Press: London, 1984.
(26) Liu, G.; Smith, C. K.; Hu, N.; Tao, J., submitted to *Macromolecules*.

MA951338U